- Technical Paper -

MESOSCALE FROST DAMAGE SIMULATION BASED ON COUPLED HEAT AND MOISTURE TRANSFER OF MORTAR WITH RBSM

Zhao WANG*1, Dawei ZHANG*2, Fuyuan GONG*3 and Tamon UEDA*4

ABSTRACT

Frost damage of mortar and concrete is an important issue for structures in some cold and wet areas. This paper presents a precise simulation work considering non-uniformly distributed moisture and heat field. Coupled heat and moisture governing equations with ice formation are applied into a discrete numerical method (RBSM). Water penetration profile and thermal lag matches the experiment evidence well. Finally, deformation and cracking at different locations of the mortar specimen due to freeze and thaw cycle (FTC) are simulated, which happens non-uniformly in target specimens.

Keywords: frost damage, coupled heat and moisture transfer, mesoscale simulation, cracking

1. INTRODUCTION

Frost action is an essential factor in cold region, and has been studied for many years. Ueda, et al proposed a mesoscale constitutive model for concrete and mortar under freezing and thawing cycles and introduced the concept of plastic tensile strain [1]. Hasan, et al carried open test for up to 300 freeze thaw cycles (FTCs) to find increasing deformations continually [2]. Meanwhile closed test by Sicat, et al showed expansion in first few cycles and contraction with increase of FTC number [3]. To explain such complex strain behavior, Gong, et al achieved a more flexible and comprehensive pressure model by combining poromechanics, hydraulic model and crystallization/cryosuction model. Mesoscale simulation was applied for uniform moisture and heat distribution cases which shows satisfactory agreement with experimental results by Sicat, et al [3, 4].

However, in real case structures, moisture and heat are not uniformly distributed thus the frost damage level varies at different locations. Some experiment evidences have shown thermal lag in large size specimen during FTCs which means the temperature differs from surface to center [2]. Even in small size specimen, great thermal lag would also take place if experiencing a fast freezing and thawing cycle [5]. Most researchers focus on the fully saturated condition. While in real structures, only those sides with the water supplement will have high enough water saturation degree that could lead to severe frost damage. This accounts for the reason that usually surface layers suffer from serious damage under FTCs.

Several studies have been conducted on the moisture transfer controlled by the coupled effect of heat and moisture concentration but freezing condition is not considered. Matsumoto introduced moisture chemical potential as an index and developed a mathematical model for coupled heat and moisture equations which also considers the ice formation [6]. In this paper, Matsumoto’s coupled transfer model will be adopted by differential method into the Rigid Body Spring Model together with internal pressure model and mechanical model under frost damage to accomplish a more general and precise simulation of frost damage in mortar [1, 4].

2. MODELS OF ANALYSIS

2.1 RBSM and Lattice model

(1) RBSM

The RBSM is a discrete numerical analysis method. RBSM is suitable for static and small deformation problems compared with other discrete numerical analysis and more proper to simulate splitting and cracking in cement-based materials such as mortar and concrete [1, 7].

The analytical model in RBSM is divided into polyhedron elements consisting of two transitional and one rotational degree of freedom at the centroid of element. Element mesh which represents a mortar or an aggregate cell is divided using Voronoi diagram based on the geometric computational software to ensure the cracks taking place in random direction. For two adjacent elements, two springs named normal spring and shear spring respectively are placed at the boundary of the elements, as indicated in Fig.1.

(2) Lattice model

In order to simulate the cracking effect on the coupled moisture and heat transfer, a refined approach of Lattice elements is proposed [7]. Transportation takes place along the one-dimensional Lattice pipe

*1 Laboratory of Engineering for Maintenance System, Hokkaido University, JCI Student Member
*2 Associate Prof., College of Civil Engineering and Architecture, Zhejiang University, Dr. E.
*3 Researcher, Dept. of Civil Engineering, University of Tokyo, Dr. E., JCI Member
*4 Professor, Laboratory of Engineering for Maintenance System, Hokkaido University, Dr. E., JCI Member

where transfer characteristic will change with the cracking propagation, as shown in Fig.2.

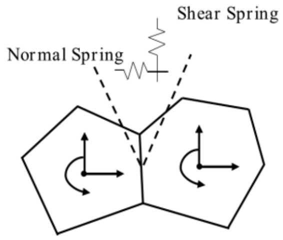

Fig.1 Elements, degree of freedom and springs

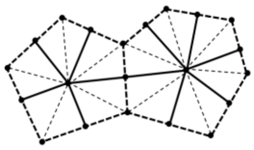

Fig.2 Schematic of lattice model

2.2 Couple moisture and heat transfer model

Coupled heat and moisture transfer equations are used to calculate the water content, ice content and temperature at any location of material [6]. Some important assumptions are adopted: 1) local equilibrium between each phase in porous media is achieved; 2) total pressure of gas phase is assumed constant which means no bulk flow of dry air takes place; 3) non-deformable porous media where stresses are kept constant and uniform are assumed; 4) chemical potential is constant for certain water content. The governing equations are given as the moisture equilibrium equation considering three phases in Eq.1 and heat equilibrium equation considering three phases in Eq.2 (proposed in [6]):

$$\frac{\partial \rho_l \psi_l}{\partial \mu}\frac{\partial \mu}{\partial t} = \nabla \bullet \left\{ \left(\lambda'_{\mu g} + \lambda'_{\mu l} \right) \nabla \mu \right\} + \nabla \bullet \left\{ \lambda'_T \nabla T \right\} - \frac{\partial \rho_i \psi_i}{\partial t} \qquad (1)$$

$$C\rho \frac{\partial T}{\partial t} = \nabla \bullet \left\{ H_{gl} \lambda'_{\mu g} \left(\nabla \mu \right) \right\} + \nabla \bullet \left\{ \left(\lambda + H_{gl} \lambda'_{Tg} \right) \nabla \mathrm{T} \right\} + H_{li} \frac{\partial \rho_i \psi_i}{\partial t} \qquad (2)$$

$$\mu_i = H_{li} ln\left(\frac{T}{T_0} \right) \qquad (3)$$

$$\psi_l = \frac{(1-k)\left[1+(C-1)k\right] exp\left(\frac{\mu}{RT}\right)}{\left[1-k exp\left(\frac{\mu}{RT}\right)\right]\left[1+(C-1)k exp\left(\frac{\mu}{RT}\right)\right]} \qquad (4)$$

where μ [J/kg] is moisture chemical potential of free water, ρ_j [kg/m^3] ($j=i,l$) is density for each phase (i for ice, l for liquid), C [J/kgK] is the specific heat, t [s] is the time, ψ_j $(j=i,l)$ [m^3/m^3] is the moisture content for each phase (i for ice, l for liquid), λ [J/smK] is the thermal conductivity, $\lambda_{\mu l}'$ [kg/ms(J/kg)] is the moisture transfer ratio in liquid phase caused by chemical potential gradient, $\lambda_{\mu g}'$ [kg/ms(J/kg)] is the moisture transfer ratio in gas phase caused by chemical potential gradient, λ_T' [kg/msK] is the moisture transfer ratio in gas and liquid phase caused by temperature gradient, λ_{Tg}' [kg/msK] is the moisture transfer ratio in gas phase caused by temperature gradient, H_{gl} [J/kg] is the evaporation heat, H_{li} [J/kg] is the melting heat. For lattice pipe along crack direction, before cracking happens, thermal conductivity and heat capacity are based on the volume fraction of mortar, ice, water and air. After cracking takes place, both factors are based on the volume fraction of ice, water and air.

Equilibrium relational expression of chemical potential and ice temperature is derived from thermodynamic analysis as Eq.3, where T [K] is the absolute temperature, T_0 [K] is the freezing temperature of free water (273.16 [K]) (proposed in [6]). To solve the four unknowns (μ, T, ψ_i, ψ_l), in the governing equations, the μ-ψ_l equation (Eq.4) is adopted based on mathematical model and chemical potential equilibrium (proposed in [8]).

2.3 Internal pressure model in porous materials

(1) Hydraulic pressure model

Two theories exist to explain the hydraulic pressure: One assumes that liquid water can flow to entrained air voids when ice forms by pressure gradient and thus generate hydraulic pressure; the other one assumes that the hydraulic pressure caused by volume increase can be balanced by the compression of water and ice instead of escaping the sealed conditions. However, in reality both theories exist depending on the distribution of empty pores and a comprehensive expression is developed and adopted, see Eq.5 (proposed in [4]). Q is the water flow by Powers' model, ϕ is the porosity, ε and ψ are the volume strain and normalized content with subscripts p,c,l for porous body, ice content and liquid respectively.

$$0.09\phi\psi_c - Q = \varepsilon_p - \phi\psi_c\varepsilon_c - \phi\psi_l\varepsilon_l \qquad (5)$$

(2) Cryosuction pressure model

Due to the surface tension, there is a pressure difference between liquid and crystal on the crystal-liquid interface as well as between the liquid and gas on the liquid-vapor interface (proposed in [11]). If assuming the pressure of gas is same as the ambient pressure (zero), then the cryosuction is always negative and depends on the temperature. T_0=0 ℃, $\Delta S_{fv}\approx 1.2$ J/cm^3·K is the molar entropy of fusion. [11].

$$p_l = \psi_l \bullet \Delta S_{fv} \bullet \left(T - T_0\right) \qquad (6)$$

(3) Crystallization pressure model

The crystallization pressure acting on the pore wall is always accompanied with the cryosuction pressure as the following equation (proposed in [11]). λ is the pore shape factor (0 for sphere pore, 0.5 for cylindrical pore). Based on Sun et al.'s experimental data, λ is regressed as λ=0.125-0.0095T [11].

$$p_c = -\psi_c \bullet \left(1-\lambda\right) \bullet \Delta S_{fv} \bullet \left(T - T_0\right) \qquad (7)$$

2.4 Mechanical model for frost damaged mortar

For porous body suffering frost damage, stress-strain relationship is adopted as Ueda, et al suggested (proposed in [1]), as shown in Fig.3. A linear unloading-reloading path when the maximum historical strain is larger than ε_0 is adopted, which follows the envelope curve in compression at a strain ε_{pa}, which equals to 171μ based on Evdon et al.'s data [3]. Internal pressure is applied on the parallel spring system (porous body as the black spring and ice-liquid system as the blue spring) instead of just the ice-liquid system because final stress and strain of the porous body which we are interested in are the same for both conditions. As shown in Fig.4 (a) and Fig.4 (b), whether adding frost action force σ_0 on ice-liquid or parallel system, the stress of porous material is σ_p. σ_p and σ_w represent the stress in porous material and ice-liquid system [4].

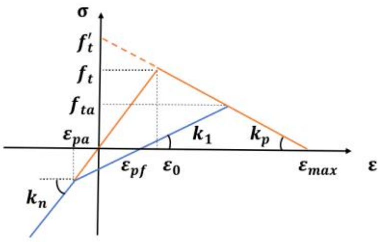

Fig.3 Stress-strain relationship for mortar

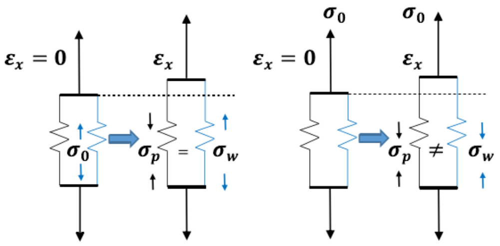

Fig.4 Parallel spring system (a) pressure internally added (b) pressure externally added

Based on the models stating above proposed by the previous researchers' studies, programing work is conducted to simulate frost damage of mortar under coupled heat and moisture transfer, which is stated in detail in the next chapter.

3. MESOSCALE SIMULATION WITH RBSM

In the simulation model for mortar case, 900 Voronoi elements are randomly meshed with 10239 lattice elements. For concrete case, 1249 Voronoi elements including mortar parts and aggregate parts are existing with 12733 lattice elements (see Fig.5). Red solid line stands for temperature chamber while blue dash line stands for water supplement boundary. Case 1 is cross section at mid-height of concrete column in FT chamber [2, 5], and Case 2 is the cross section in longitudinal direction where water penetrating [9, 10].

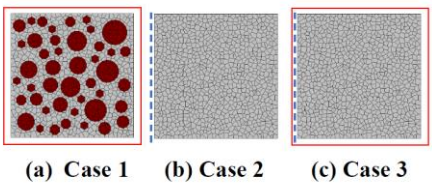

Fig.5 Boundary conditions and specimen mesh

In thermal transfer equation, heat capacities are set generally as 930, 4100, 2100 and 1000 [J/kg/K] for porous material, water, ice and air, respectively with corresponding thermal conductivity of 1.35, 0.6, 2.2 and 0.02 [J/s/m/K] respectively.

$$D = \left(\frac{S}{\theta_s - \theta_i}\right)^2 \cdot \frac{\exp(6\theta)}{123.131} \tag{8}$$

For moisture transportation, water diffusivity is used instead of permeability since the water penetration into an unsaturated specimen is driven by capillary suction (chemical potential gradient) instead of external pressure [7]. A simplified empirical equation is adopted as Eq.8, in which S [mm/min$^{0.5}$] is the sorptivity of porous material and can be obtained experimentally, θ_s and θ_i are equal to the porosity of the concerned material and 0 respectively, and θ represents the relative water content. For water transporting along the lattice pipe of crack direction, water diffusivity D is set to be 10^5 mm^2/day after cracking takes place [12].

During calculation, a combined conductivity depending on component of the mixture is adopted. A differential method is adopted to calculate the coupled equation on lattice elements with time step of 0.05s to ensure simulation convergence which is followed by mechanical calculation. Before cracking, width of the boundary lattice model is set as zero and after cracking is set according to the normal spring deformation once the mechanical calculation is finished.

3.1 Outline of temperature transfer simulation

To evaluate the temperature transfer and thermal lag phenomenon of porous materials in a freezing and thawing temperature chamber, simulation of concrete is conducted and compared with some experimental evidence. Boundary condition is shown in Fig.5 (a): all sides of the square concrete specimen are set with a freezing/thawing temperature change without any water supplement. FTC is set from maximum 20 ℃ to minimum -20 ℃ then back to maximum in 3 freezing speed (15, 20[2] and 25[5] ℃/h) on 3 sizes of concrete specimen (100x100[5], 200x200 and 300x300[2] mm). Among, the experiments with the same sizes and freezing speeds are modeled for temperature evaluation. A relationship between thermal lag and freezing speed/size is also given based on the simulation results.

3.2 Outline of water transfer simulation

In order to check the water penetration profile, initially fully dried mortar specimen (100x100 mm for all models) is analyzed. One side of the mortar faces water supplement while other sides have no water transfer with external space, as shown in Fig.5 (b). Water diffusivity can be calculated based on the test value of porosity and sorptivity (see Table 1).

Table 1 Water transfer characteristics

Experiment	Porosity-φ	Sorptivity-S (mm/min^2)	Diffusivity-D (mm^2/min)
Hall, 1989	0.27	2.57	0.736
Carpenter, 1988	0.239	1.00	0.142

All the penetration process happened in the room temperature without FT change. After certain time, water penetration profile is checked and compared with previous experimental data.

3.3 Frost damage under coupled transfer

Finally, both conditions (FTC chamber and water supplement) are given to the mortar specimen (100x100 mm) to analyze the frost damage under coupled effect of heat and moisture transfer, as shown in Fig.5 (c).

Specimen named MD is initially fully dried mortar. Water penetrates from the left face and FT temperature change takes place in all four faces simultaneously. While specimen named MS and MSL are fully saturated cases with only freezing and thawing temperature change in all sides. Water transfer conductivity of both specimens is given as Hall's experimental data. In order to analyze the effect of specimen size, initial moisture condition and boundary condition on the frost damage, a typical FTC is set for specimen MD, MS and MSL, as shown in Fig.6. Temperature of the boundary elements will follow the FTC curve, while temperature of the rest elements are calculated based on the coupled equations.

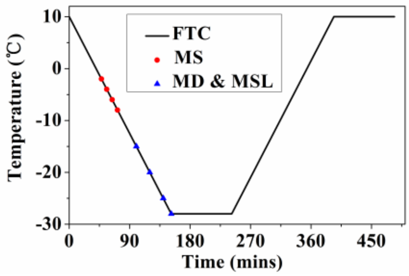

Fig.6 A typical FTC curve

4. RESULTS AND DISCUSSION

4.1 Temperature distribution and thermal lag

RBSM simulation model for heat transfer only is compared with experimental evidence and showing a satisfactory agreement which supports the utilization of thermal transfer model and lattice model, as shown in Fig.7 and Fig.8 [2, 5], where "E" means experimental data and "S" stands for simulation result.

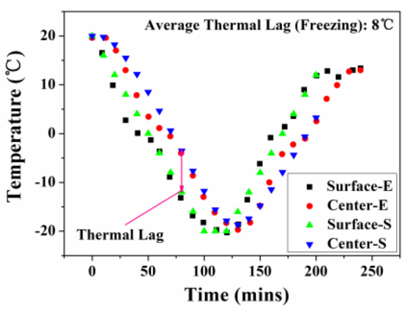

Fig.7 Comparison with Bishnoi's experiment

Based on experimental and simulation results, for 100x100 mm concrete specimen subjected to a freezing speed of 25 ℃/h, the average thermal lag is 8 ℃ between surface and center part. While for 300x300 mm concrete specimen subjected to a freezing speed of 20 ℃/h, the average thermal lag is 20 ℃.

It evident that an obvious thermal lag between different locations of concrete exists under freezing and thawing cycles. From both experiment and simulation results, it can be indicated that larger size and faster freezing speed will lead to a more serious thermal lag. Besides, size effect shows more obvious effect on the thermal lag phenomenon than the freezing speed does, as shown in Fig.9.

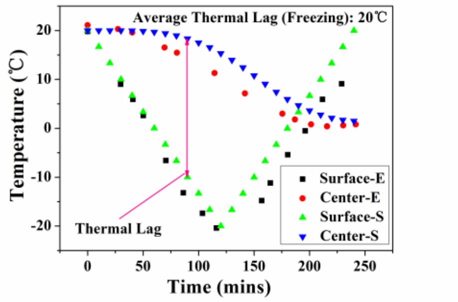

Fig.8 Comparison with Hasan's experiment

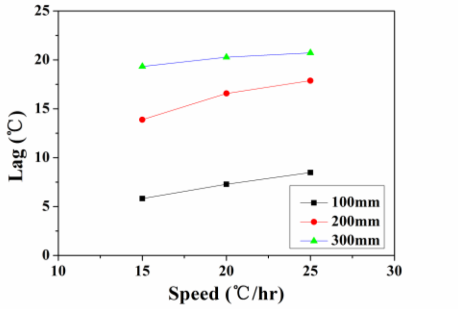

Fig.9 Freezing speed – thermal lag relationship

4.2 Water penetration profile

The water penetration profiles under temperature above freezing point predicted by the lattice model in RBSM are shown in Fig.10 and Fig.11 to compare with experiment results by Hall in 1989 and Carpenter in 1988 [9, 10]. Boltzmann variable φ ($\varphi = xt^{0.5}$) is used as an index when evaluating the water penetration profile [7].

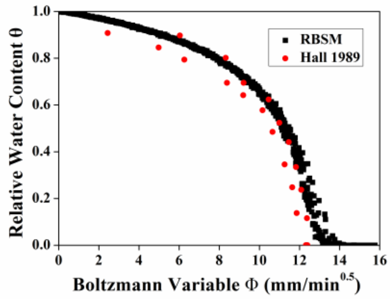

Fig.10 Comparison with Hall's experiment

It is found that the predicted results can match very well with the experimental data and therefore support the reliability of applying the moisture transfer model together with the lattice model to water penetration analysis.

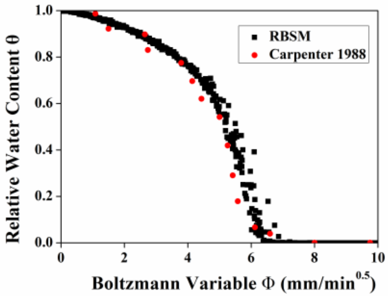

Fig.11 Comparison with Carpenter's experiment

4.3 Deformation and crack under coupled transfer

After both the heat and moisture profiles have been evaluated, a coupled heat and moisture transfer effect on frost damage of mortar is simulated. Red line between two elements means crack has taken place.

During FTC and water penetration, strains are calculated in surface part, inner part as well as the whole specimen span to record the deformations at different locations. For one freezing and thawing cycle, the predicted cracking propagation is given as a visual way to evaluate the frost damage. Certain time are picked as shown in blue and red dots drawn in Fig.6.

Model MS in Fig.12 indicates that in initially fully saturated case, the thermal lag will affect the time of ice formation at different locations. The surface part will suffer a faster ice formation and thus earlier damage. Due to the thermal lag (around 5 ℃ between surface and center elements), the center part of mortar will never reach as high frost pressure as surface part.

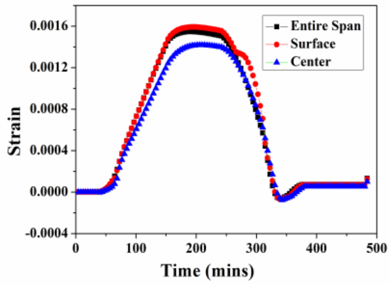

Fig.12 Strain – time curves for MS in typical FTC

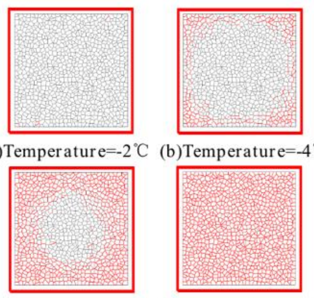

Fig.13 Crack propagation in certain steps for MS

The predicted cracking (springs that reach the cracking criterion) propagation in specific steps where boundary temperature equals to -2, -4, -6 and -8 ℃ (see Fig. 6) is given for one freezing and thawing cycle. As shown in Fig.13, it indicates that the cracks develop from the surface part which suffers freezing earlier than the inner part due to the thermal lag.

For initially dry case MD, even when the temperature reaches freezing point, most inner parts are still in a low saturation degree as a result of the short water penetrating duration, only the surface parts suffer severe damage (see Fig.14). During the FTC, surface parts are in tension force due to ice formation while inner parts are in contraction force.

The cracking propagation in specific steps where boundary temperature equals to -15, -20, -25 and -28 ℃ (see Fig. 6) is also given for model MD. Figure 15 indicates that the cracks only take place in the surface parts. Most severe damage can be seen along the side exposed to water, followed by the top and bottom boundaries.

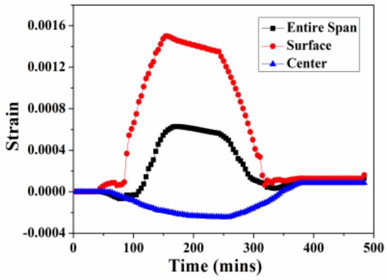

Fig.14 Strain – time curves for MD in typical FTC

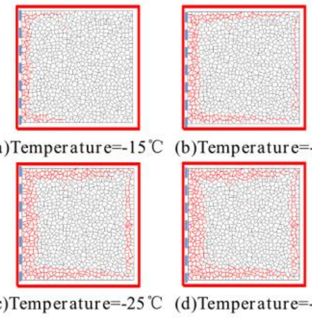

Fig.15 Crack propagation in certain steps for MD

The side far from water supply also suffers frost damage since the saturation degree has been high enough due to the fast water penetration before temperature reaches freezing point. Most inner parts do not generate any cracking, this is because once the surface parts have ice formation, chemical potential will decrease [8], water from inner parts will flow to the void in these surface parts to reach an equilibrium. This lead to lower saturation in the inner parts, also thermal lag exists (≈5 ℃), the inner parts don't have damage.

Besides, to evaluate the effect of thermal lag on large size specimen, a special model of 300x300 mm mortar (MSL) was simulated with initially fully saturated condition (thermal lag≈20 ℃). The cracking propagation in specific steps where boundary temperature equals to -15, -20, -25 and -28 ℃ (see Fig. 6) is given, as shown in Fig. 16. Relative damaged depth (crack reaching length/ half specimen length) is adopted as an index to evaluate the thermal lag effect on cracking propagation during temperature decreasing for saturated mortar specimen MS and MSL (Fig. 17).

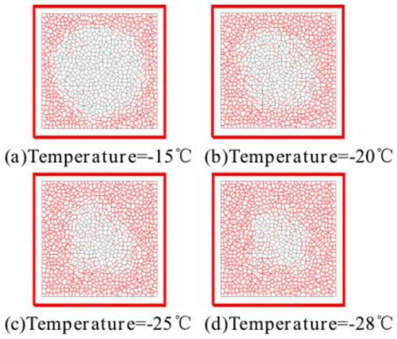

Fig.16 Crack propagation in certain steps for MSL

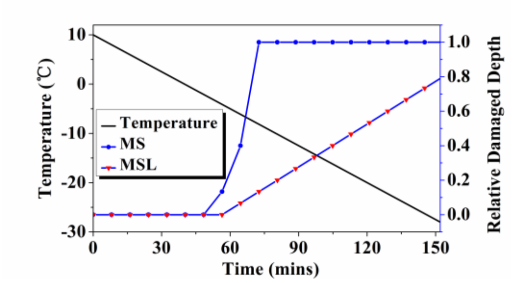

Fig.17 Relative damaged depth of MS and MSL

5. CONCLUSIONS

(1) In this paper, a more precise analytical method of properties of mortar as porous material is given when the porous materials suffers from frost damage action. Based on the coupled heat and moisture transfer equations, the non-uniformly distributed temperature and moisture content can be calculated. Combining the temperature and moisture coupled field with the frost damage model, the internal pressure, deformation and cracking distribution was be determined. Since such precise observation in experiment is still hard to conduct, this simulation can give an efficient way to predict the frost damage in concrete structure level.

(2) From the numerical simulations in this paper the following conclusions on the effects of specimen size, initial moisture condition and boundary conditions can be drawn:

- For fully saturated mortar specimen with size of 100x100 mm, surface parts will suffer internal pressure earlier than the inner parts due to thermal lag. For larger size of mortar with size of 300x300 mm suffering same FTC, only surface layer suffers freezing temperature thus severe damage due to large scale of thermal lag. As well-known points, the phenomenon stated above is simulated successfully based on the coupled equations.
- For fully dry mortar specimen with size of 100x100 mm, with water penetration and temperature decrease, surface of mortar will have severe damage. Sides exposed to the water will usually have more cracking. The whole specimen shows a contraction instead of expansion.

ACKNOWLEDGEMENT

This study was conducted under the Grant-in-Aid for Scientific Research (A) of Japan Society of Promotion of Science (No. 26249064).

REFERENCES

[1] Ueda, T., et al., Mesoscale Simulation of Influence of Frost Damage on Mechanical Properties of Concrete. Journal of Materials in Civil Engineering, 2009. 21(6): p. 244-252.
[2] Hasan, M., Okuyama, H. and Ueda, T., The Damage Mechanism and Strain Induced in Frost Cycles of Concrete. Proceedings of JCI, 2003. 25(1): p. 401-406.
[3] Sicat, E., et al., Change of the Coefficient of Thermal Expansion of Mortar Due to Damage by Freeze Thaw Cycles. Journal of Advanced Concrete Technology, 2013. 11(12): p. 333-346.
[4] Gong, F., et al., Physical Model and Mesoscale Simulation of Mortar and Concrete Deformations under Freeze–Thaw Cycles. 4th International Conference on the Durability of Concrete Structures, 2014.
[5] Bishnoi, S. and T. Uomoto, Strain–temperature Hysteresis in Concrete under Cyclic Freeze–thaw Conditions. Cement and Concrete Composites, 2008. 30(5): p. 374-380.
[6] Matsumoto, M., S. Hokoi, and M. Hatano, Model for Simulation of Freezing and Thawing Processes in Building Materials. Building and Environment, 2001. 36(6): p. 733-742.
[7] Wang, L. and T. Ueda, Mesoscale Modeling of Water Penetration into Concrete by Capillary Absorption. Ocean Engineering, 2011. 38(4): p. 519-528.
[8] Gong, F., et al., Empirical Estimation of Pore Size Distribution in Cement, Mortar, and Concrete. Journal of Materials in Civil Engineering, 2013. 26(7): p. 04014023.
[9] Hall, C. Water Sorptivity of Mortars and Concretes: A Review. Magazine of Concrete Research, 1989. 41, p. 51-61.
[10] Carpenter, T.A., et al., Capillary Water Migration in Rock: Process and Material Properties Examined by NMR Imaging. Materials and Structures, 1993. 26(5): p. 286-292.
[11] Sun, Z., et al., Effect of air voids on salt scaling and internal freezing, Cement and Concrete Research, 2010, 40(2): p. 260-270.
[12] Nakamura, H., et al., Time-dependent structural analysis considering mass transfer to evaluate deterioration process of RC structures, Journal of Advanced Concrete Technology, 2006, 4(1): p. 147–158.